DOI: 10.13009/EUCASS2019-105

Numerical Simulations of an Isochoric Hybrid Rocket Combustion Chamber and Comparison with Tests

F. Barato, E. Paccagnella*, G. Venturelli*, D. Pavarin*, F. Picano* and J-Y Lestrade***
**Department of Industrial Engineering, University of Padua*
Via Venezia 59/4, Padua, Italy, 35131, francesco.barato@unipd.it
***ONERA - The French Aerospace Lab,*
F31410 Mauzac, France, Jean-Yves.Lestrade@onera.fr

Abstract
Conventional hybrid rocket motors are not suitable for low thrust, very long burning time spacecraft applications because of the time-dependent shift in mixture ratio and associated variations in grain shape. In the Framework of the European Commission's H2020 HYPROGEO program, an innovative combustion chamber has been proposed to explore the application of hybrid propulsion as a replacement for current liquid propellant apogee engines. Such a combustion chamber, which is isochoric, has a length-to-diameter ratio of the order of one. This unconventional hybrid rocket is based on an end-grain solid fuel burning axially in conjunction with a lateral swirled injection of oxidizer.
To support the development of this new architecture of hybrid engine a customized commercial CFD code has been used by University of Padua to perform multiple simulations with the aim of understanding the combustion behaviour in the isochoric chamber and predicting the main motor parameters like regression rate and wall heat transfer. Meanwhile, an experimental campaign on the new motor design has been prepared and executed by ONERA.
The paper will consequently present the numerical simulations performed and the comparison with the experimental tests. The result of the investigation is that the isotropic turbulence model chosen for the standard simulations is not fully compatible with the selected swirled injection, while more advanced models can describe better the local flowfield, particularly at the axis of the combustion chamber. However, the isotropic model is still able to predict with reasonable accuracy the global performance of the motor.

1. Introduction

Conventional hybrid rockets are not suited for low thrust-very long burning time applications because of too high O/F shift and unreasonable grain shape. To extend the application of hybrid propulsion as replacement of current liquid apogee engines an isochoric combustion chamber solution has been proposed by Airbus Defence & Space and ONERA. This unconventional hybrid rocket, based on a solid fuel burning axially and a lateral oxidizer injection, has been developed in the frame of the H2020 HYPROGEO program [1-3]. The role of University of Padua in HYPROGEO was to perform the numerical simulations to support the other partners in the design of the motor.
In Work Package 2 UNIPD was responsible to perform the numerical simulations of the HYPROGEO hybrid motor combustion chamber. UNIPD has used a commercial software customized by UNIPD for the specific purpose of simulating hybrid rocket motor combustion [4]. These numerical tools have been previously validated with experimental results of classical hybrids, mainly Carmicino et al. [5-8]. These tools have been used in HYPROGEO to simulate the so-called ONERA piston concept in order to understand the internal fluidynamic and optimize the design, particularly the injection scheme. The piston concept foresees an end burning cylindrical grain that is continuously pushed axially in order to keep a constant combustion chamber volume (i.e. isochoric chamber). In principle, this concept overcomes the typical difficulties incurred by classical hybrids for very long burns providing constant burning conditions with time. The great challenge of this configuration is to obtain a high combustion efficiency together with a very low regression rate necessary to obtain a reasonable grain length to diameter ratio. The regression rate has also to be spatially uniform to guarantee constant burning conditions with time.
A previous paper addressed the preliminary simulations of the isochoric combustion chamber for ONERA critical design progress [9]. At the beginning, several simulations have been performed with the aim of understanding the behavior of the combustion in the proposed isochoric chamber. Preliminary simulations have been done imposing the fuel mass flow according to the target regression rate. Several injection positions and parameters have been studied.

DOI: 10.13009/EUCASS2019-105

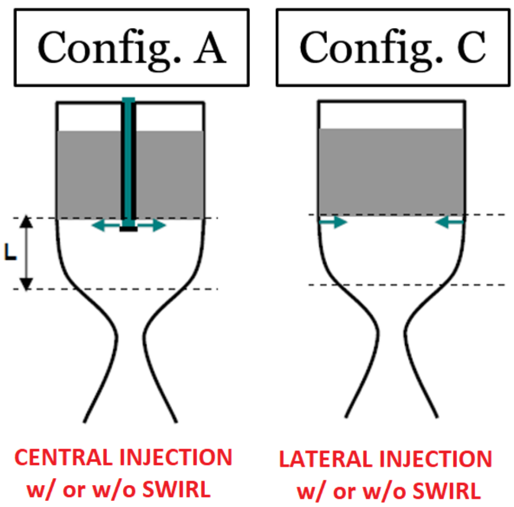

Figure 1: Injection positions

Straight lateral injection (config. C) produces too low efficiencies but also a low thermal load for the chamber walls because the flame is located in the central part of the combustion chamber. On the opposite, central injection (config. A) induces higher efficiencies but very high heat transfer to the chamber walls because of the flame position on the outer periphery. Adding a swirled flow always increases the efficiency and heat transfer. Moreover, the efficiency increases with the inlet oxidizer flux. Finally, simulations have been performed without imposing the fuel regression rate, this quantity being calculated with a user-defined function from the heat transfer on the grain surface. Variations of performances with scale and throttling of the oxidizer mass flow have been also investigated. The preliminary simulations of the piston concept performed by UNIPD in the first year of the HYPROGEO program were useful to understand the basic combustion flow and performance of the engine and compare different configurations and parameters. At the end of this preliminary investigation, the lateral swirl injection has been determined to be the best solution has a trade-off between efficiency, thermal load, regression rate uniformity and injector complexity.

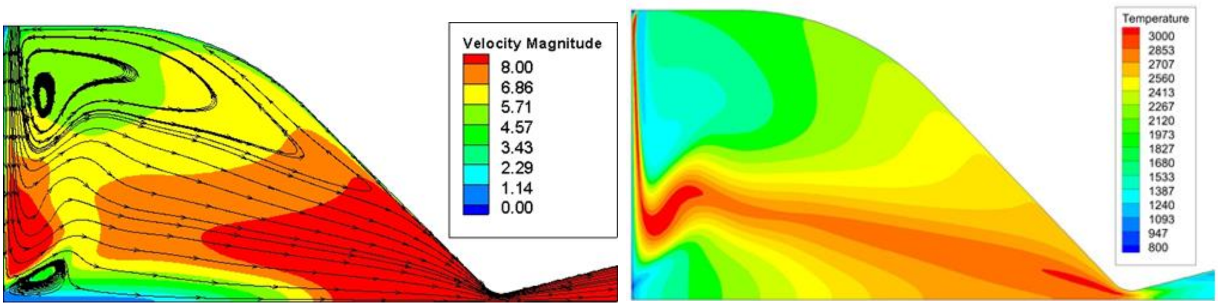

Figure 2: Lateral swirl injection, velocity (left) and temperature (right) profiles

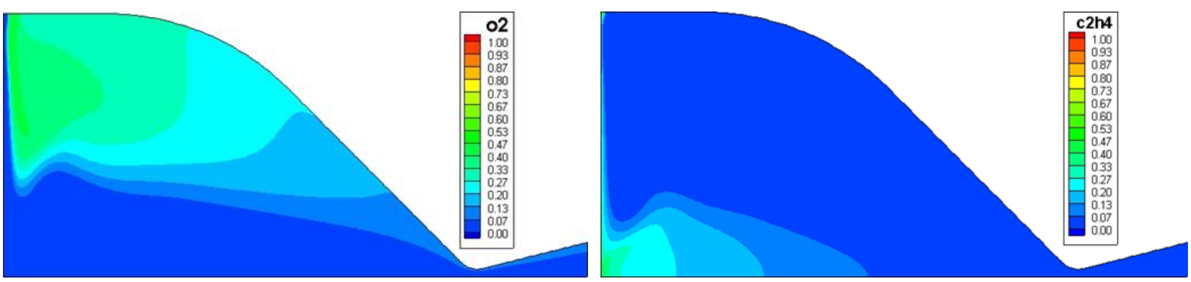

Figure 3: Lateral swirl injection, oxidizer (left) and fuel (right) mass fractions

In order to reduce the computational time, the initial simulations of the HYPROGEO combustion chamber for the piston configuration were performed using a 2D axisymmetric condition. In this case, the oxidizer was injected in a

DOI: 10.13009/EUCASS2019-105

small ring on the lateral chamber surface near the fuel surface. However, the real injector had a more complicated design that is not fully axisymmetric even if it keeps a certain periodicity. In order for DELTACAT and ONERA to define the more suitable injector design, some specific simulations have been performed by UNIPD in the second year of HYPROGEO. In this case, fully 3D computations have been executed. Those CFD calculations were needed to explore the quality of the flow within the combustion chamber, in particular the variation of the flame and the heat flux on the fuel grain along the circumferential and radial directions caused by the specific injector geometry.

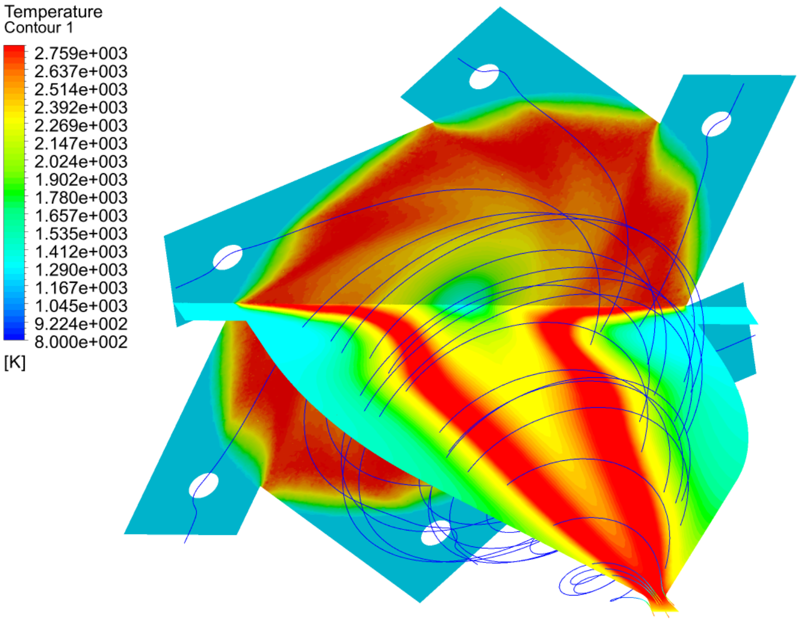

Figure 4: Full three dimensional simulation of the HYPROGEO hybrid motor

After that, other 2D and 3D simulations were performed by UNIPD to help the design of the final breadboard. In particular, some simulations were executed in order to determine the heat transfer to the chamber walls for different selections of some motor parameters. These simulations were needed in order to help VKI/ONERA in determining the temperature reached by the combustion chamber walls and verify the thermal design. The results of the heat transfer analyses are presented in section 3.
Finally, after the first experimental campaign performed by ONERA on the initial breadboard the numerical results have been compared to the ones retrieved by the ONERA experimental tests. Some discrepancies, particularly in the local values of fuel consumption behavior have been found and investigated in the last year by means of 2D and 3D simulations, finally determining that they were related to the selected turbulence model. However, the original model showed to be still able to predicts the global performance of the motor. The results of the comparison are presented in section 4.

2. Simulation set-up

All the simulations had the following characteristics.
Simulation type: steady state, pressure based, coupled;
Discretization mode: second order;
Turbulence model: K-ω SST (except in the last section where there are also simulations using the Reynolds Stress equation Model, RSM);
Combustion model: eddy dissipation (suitable when kinetics is fast compared to mixing [10]);
Chemical reaction:

$$392\ C_2H_4 + 1049\ O_2 \rightarrow 188\ CO + 128\ H_2 + 594\ H_2O + 124\ OH \tag{1}$$

Boundary conditions: outlet at nozzle exit, fuel inlet at the grain surface (with or without UDF), oxidizer inlet at the base of the injectors and adiabatic or fixed temperature walls for the chamber walls. The adiabatic wall condition was used for the basic understanding of motor behavior/performance, while the fixed temperature condition was used specifically to determine the heat transfer to the chamber walls.

DOI: 10.13009/EUCASS2019-105

Both the oxidizer (Hydrogen Peroxide) and the fuel (Polyethylene) were injected as their decomposed gaseous products (Oxygen and Water, Ethylene, respectively) at 1223 K and 800 K, respectively. In case the UDF (User Defined Function) is used, the fuel inlet temperature is determined by the code.

The UDF uses the following equations.
Heat balance at the fuel surface:

$$\dot{r} = \dot{Q}_{wall}/\rho_f h_v \tag{2}$$

And pyrolysis of the fuel:

$$\dot{r} = Ae^{-E_a/RT_s} \tag{3}$$

Where T_s is the fuel surface temperature and:

$$h_v = h_v(T_s) \tag{4}$$

It is worth noting that if $E_a \to \infty \Rightarrow T_s, h_v \to$ cost and only the first equation is needed as it is done in simplified approaches. However, the complete set of equations is used in this case.
The wall heat transfer is the sum of a convective and a radiative term:

$$\dot{Q}_{wall} = \dot{Q}_c + \dot{Q}_r \tag{5}$$

The convective heat transfer to the wall surface is calculated by the CFD code from the temperature profile in the gas phase near the fuel surface:

$$\dot{Q}_c = -\lambda \frac{\partial T}{\partial y}\bigg|_{y=0} \tag{6}$$

A radiative term could be added as:

$$\dot{Q}_r = \varepsilon_f \varepsilon_g \sigma T_g^4 \tag{7}$$

Where *g* refers to the gas and *f* to the fuel. However, the fuel emissivity is dependent on pressure and soot production. Polyethylene does not produce much soot as HTPB and the HYPROGEO motor is designed to work at low pressures so the radiative term has been considered negligible. This is confirmed by the very low regression rate measured in the experiments.
For the convergence of the simulations, both the variation of some average values on the domain and the value at some specific points are checked. If the values do not change anymore, the simulations are stopped. The simulation is considered successful if the fluid domain makes sense and residuals (RMS) are generally between 10^{-5} - 10^{-7} depending on the variable. The equations are solved iteratively with some relaxations factor that are tuned to improve convergence.

3. Simulations for the determination of the heat transfer to chamber walls

UNIPD performed a series of 2D simulation for ONERA/VKI with the aim of determining the heat transfer to chamber walls in order to help in the design of the combustion chamber/nozzle assembly. The simulations considered different chamber diameters from 200 to 350 mm. Oxidizer mass flow rate was 70 g/s, oxidizer-to-fuel ratio was fixed to 7.4. Nozzle throat diameter was 12 mm for a theoretical pressure of 10 bar. For each geometry, UNIPD performed four simulations: one with adiabatic wall condition, the other three with fixed temperature condition: 900 K, 1000 K and 1100 K respectively. Those temperatures were in the range expected for safe motor operation with the selected materials. From the first simulation, it was possible to obtain the adiabatic wall temperature. From the other three, three different values of the wall heat transfer.
In this way, it was possible for VKI to infer the heat transfer coefficient α by the following equation:

$$\alpha = \dot{Q}_{wall}/(T_{adiabatic\_wall} - T_{wall}) \tag{8}$$

DOI: 10.13009/EUCASS2019-105

The heat transfer coefficient resulted to be nearly independent on the wall temperature in the range considered. Based on this heat transfer coefficient estimation, VKI was able to calculate the expected wall temperature depending on the wall chamber thickness and material choice.

		Main			ox-h2o2		fuel		Injection			Nozzle	Cc wall bc	
Case ID		Diam. Chamber	GOX	O/F	Concent.	mdot OX	Type	mdot FUEL	Type	Angle	Length	Diameter	type	T
[-]		[mm]	[kg/(s m^2)]	[-]	[%]	[g/s]	[-]	[g/s]	[-]	[deg]	[mm]	[mm]	[-]	[K]
TN100		200	10	7,4	98	70	c2h4	9,46	laterl - swirl	45	11,141	12	adiabatic	n.d.
TN101		200	10	7,4	98	70	c2h4	9,46	laterl - swirl	45	11,141	12	heat flux	900
TN102		200	10	7,4	98	70	c2h4	9,46	laterl - swirl	45	11,141	12	heat flux	1000
TN103		200	10	7,4	98	70	c2h4	9,46	laterl - swirl	45	11,141	12	heat flux	1100
TN90		400	12	7,33	98	176	c2h4	24	laterl - swirl	45	11,671	12	adiabatic	n.d.
TN91		400	12	7,33	98	176	c2h4	24	laterl - swirl	45	11,671	12	heat flux	900
TN92		400	12	7,33	98	176	c2h4	24	laterl - swirl	45	11,671	12	heat flux	1000
TN93		400	12	7,33	98	176	c2h4	24	laterl - swirl	45	11,671	12	heat flux	1100
TN110		350	10	7,4	98	70	c2h4	9,46	laterl - swirl	45	6,366	12	adiabatic	n.d.
TN111		350	10	7,4	98	70	c2h4	9,46	laterl - swirl	45	6,366	12	heat flux	900
TN112		350	10	7,4	98	70	c2h4	9,46	laterl - swirl	45	6,366	12	heat flux	1000
TN113		350	10	7,4	98	70	c2h4	9,46	laterl - swirl	45	6,366	12	heat flux	1100
TN120		250	10	7,4	98	70	c2h4	9,46	laterl - swirl	45	8,913	12	adiabatic	n.d.
TN121		250	10	7,4	98	70	c2h4	9,46	laterl - swirl	45	8,913	12	heat flux	900
TN122		250	10	7,4	98	70	c2h4	9,46	laterl - swirl	45	8,913	12	heat flux	1000
TN123		250	10	7,4	98	70	c2h4	9,46	laterl - swirl	45	8,913	12	heat flux	1100
TN130		300	10	7,4	98	70	c2h4	9,46	laterl - swirl	45	7,427	12	adiabatic	n.d.
TN131		300	10	7,4	98	70	c2h4	9,46	laterl - swirl	45	7,427	12	heat flux	900
TN132		300	10	7,4	98	70	c2h4	9,46	laterl - swirl	45	7,427	12	heat flux	1000
TN133		300	10	7,4	98	70	c2h4	9,46	laterl - swirl	45	7,427	12	heat flux	1100

Table 1: Summary of the simulated cases for the heat transfer analyses

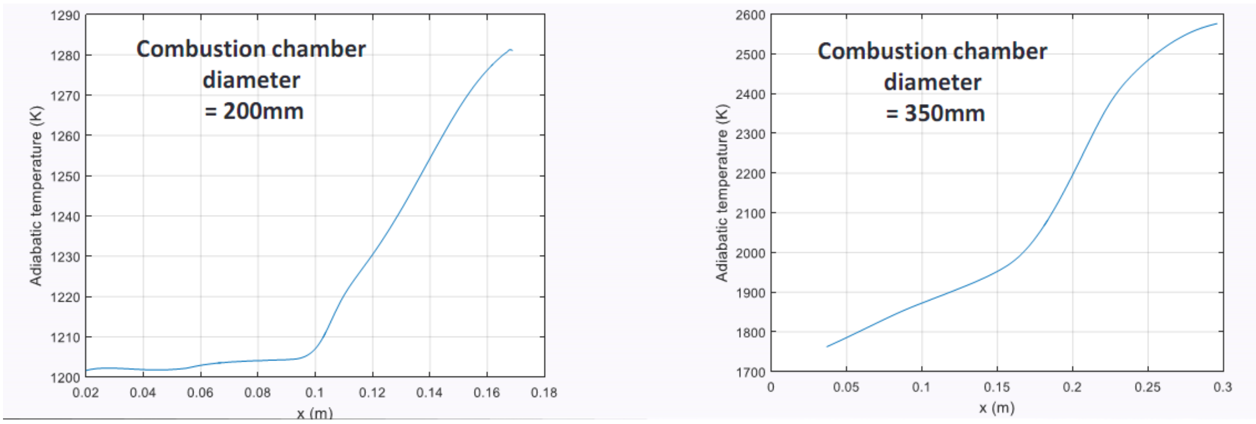

Figure 5: Adiabatic wall temperature calculated from UNIPD simulations

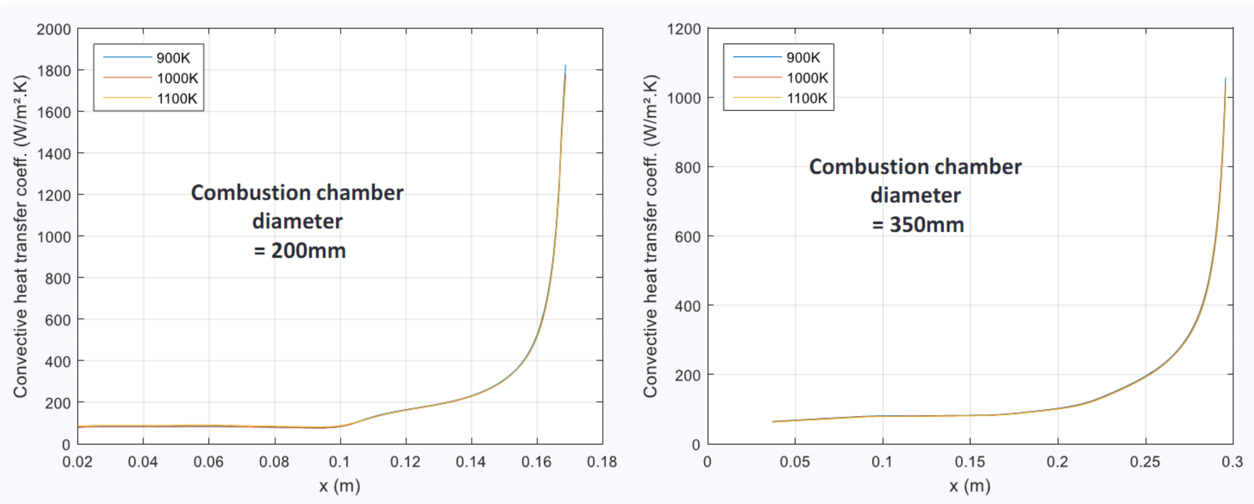

Figure 6: Convective wall heat transfer determined by VKI from UNIPD simulations

DOI: 10.13009/EUCASS2019-105

4. Comparisons with ONERA experiments on MHYCAS engine

In the autumn of 2016, ONERA performed some experiments with the initial HYPROGEO breadboard called MHYCAS. After the test campaign of the MHYCAS engine there was the opportunity to compare the experimental results with numerical predictions. UNIPD performed a full 3D simulation of the intermediate breadboard engine with the same hypotheses used in all the previous simulations. The regression rate was calculated with the same User Defined Function (UDF) developed and validated by UNIPD before the HYPROGEO program for conventional geometry hybrid rocket motors.

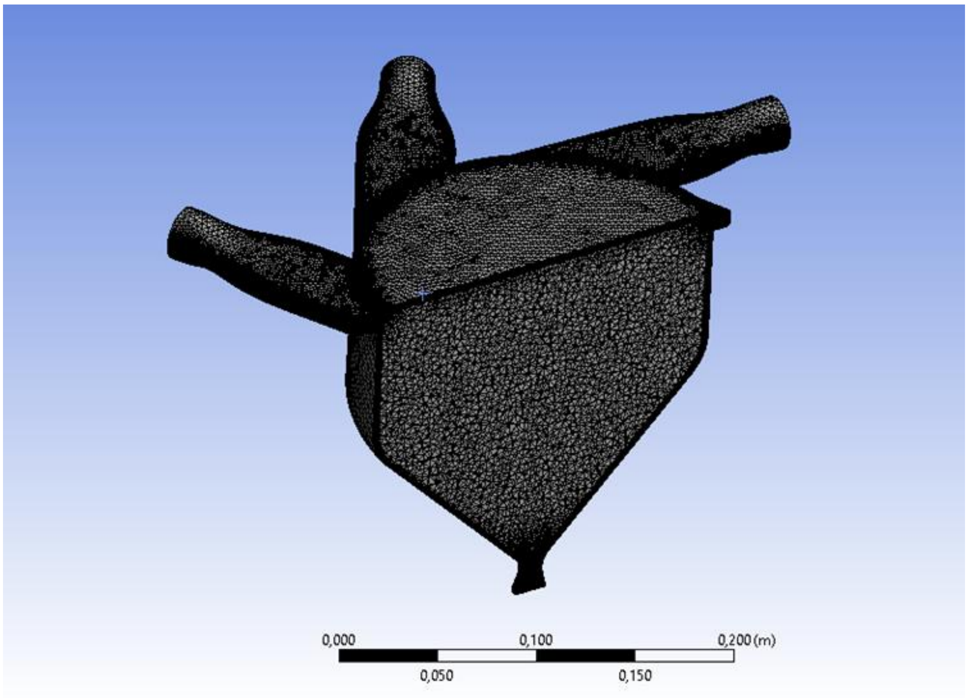

Figure 7: Mesh for the MYCHAS engine geometry

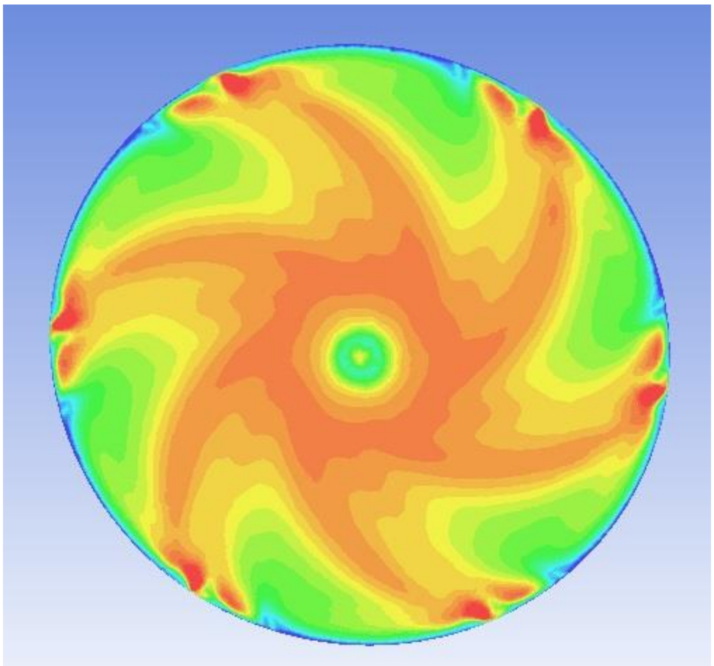

Figure 8: Adimensional regression rate on fuel surface (red max, blue min) of the MYCHAS engine geometry

DOI: 10.13009/EUCASS2019-105

After calibration of the numerical model, it was found that the main discrepancy between the experiments and the simulations was related to the behaviour of the regression rate near the centre of the fuel surface. In the experiments the regression rate peaks at the centre of the fuel surface while in the simulation there is a minimum at the same place. The peak of regression rate is confirmed also by other experiments performed outside the HYPROGEO program for similar configurations (swirled injection engines with a flat fuel surface [11]). It is assumed that this behaviour is fluidynamic and related to a recirculation near the fuel centre. The UNIPD simulation catches the recirculation at the fuel centre, but this recirculation does not contain hot temperature combustion products so it does not produce an intense heat flux. The reason for this has been related to the turbulence model. The turbulence model used in all the simulations was the K-ω SST. This turbulence model is widely used in engineering applications because of its general optimal compromise between accuracy, robustness and computational time. This model is called isotropic because it follows Boussinesq approximation where the turbulence viscosity is a scalar quantity not dependent on the direction (i.e. isotropic).

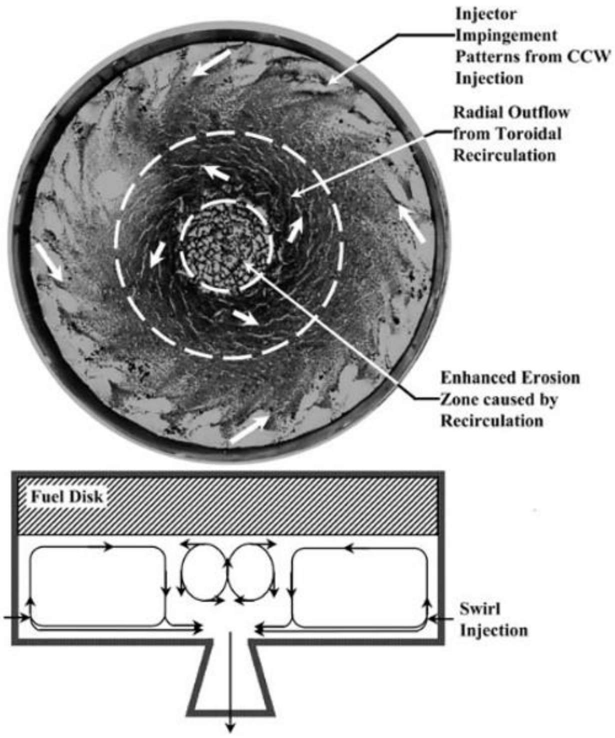

Figure 9: Previous experiment of a similar hybrid motor configuration (from [11]).

Figure 25 is a photograph of one of the Rice et al. recovered fuel disks [56]. Note the swirl pattern evident on the fuel surface. Rice et al. found that a region of very high regression rates existed near the center of the fuel disks such that the recovered fuel samples were bowl-shaped about the chamber axis. In addition, an intermediate zone of apparent counter-rotation was evident from the recovered fuel disks. The researchers postulated that this patterning actually resulted from a corotating, but radial *outflow* zone of toroidal recirculation about the chamber axis, as illustrated in the qualitative streamline plot shown in the lower portion of Fig. 25. Though they considered nonreacting situations, Georgantas et al. [65] have found that such recirculation zones are likely to exist in confined swirling flows when the swirl strength exceeds a threshold value of about 0.6, where the swirl strength is defined as

$$Sw = \frac{\dot{m}_{\mathrm{sw}} V_{\mathrm{inj}} R_c}{\dot{m}_{\mathrm{tot}} V^* R^*} = \frac{\text{input} \cdot \text{angular} \cdot \text{momentum}}{\text{exit} \cdot \text{linear} \cdot \text{momentum} \times \text{exit} \cdot \text{radius}} \tag{71}$$

Figure 10: Description of previous experiments of a similar hybrid motor configuration (from [11]).

DOI: 10.13009/EUCASS2019-105

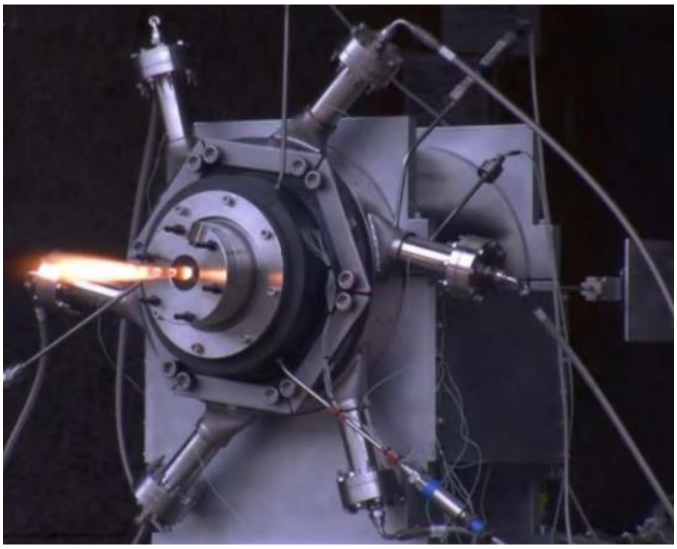

Figure 11: Fire test of the MHYCAS engine at ONERA premises

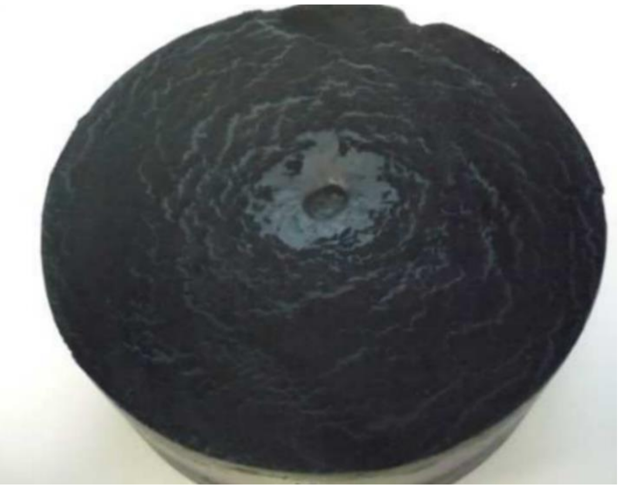

Figure 12: MHYCAS fuel grain after testing: note the presence of a peak consumption in the centre of the grain

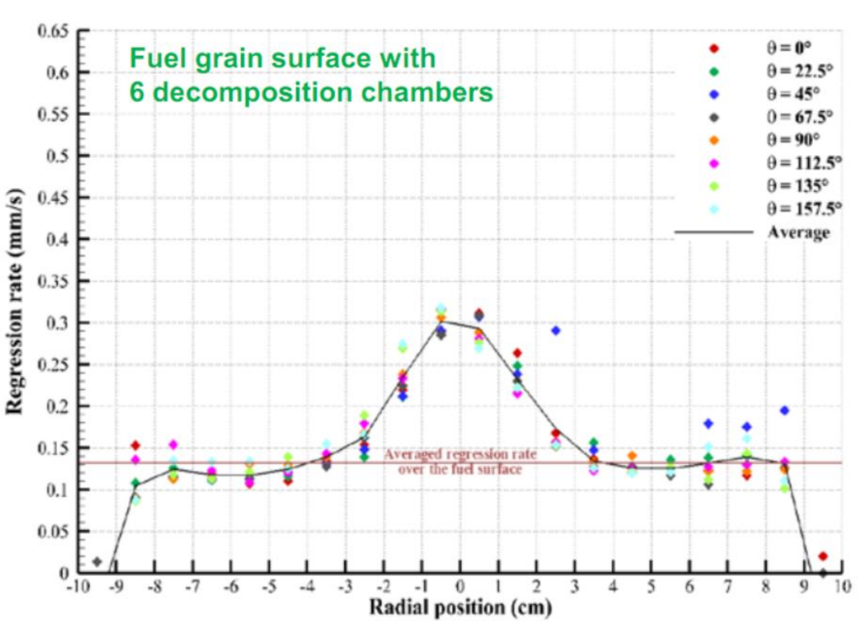

Figure 13: MHYCAS fuel regression rate distribution

DOI: 10.13009/EUCASS2019-105

However, in case of strong swirled flows, turbulence has been shown to be anisotropic and the conventional two equations models start to fail. To assess the influence of the turbulence model a preliminary investigation has been performed with a more general turbulence model, the Reynolds Stress Model (RSM). In this model, the six independent Reynolds stresses are solved. It is the most complex turbulence model for RANS (Reynolds averaged Navier Stokes). We started to compare non-combustive simulations of the breadboard with the standard turbulence model and the non-isotropic turbulence model. From the preliminary results, the new simulation are able to catch the peak at the centre of the engine. The standard model produces too much viscosity and too less turbulence near the centre compared with the non-isotropic model.

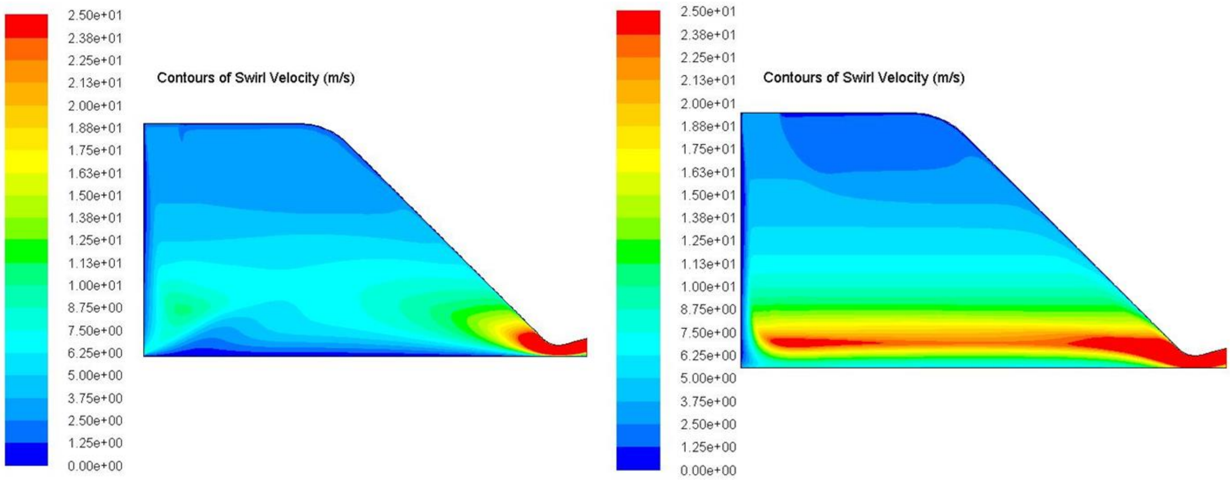

Figure 14: Swirl velocity, comparison between different turbulence models: K-ω SST (left), RSM (right)

The results of the two simulations are similar far from the axis of the engine. As the centre is approached, the tangential (swirl) velocity has to increase for the conservation of angular momentum. At the axis, the inviscid flow predicts a singularity of infinite velocity. In the real case, the fluid viscosity dampen the flow and the velocity reaches a peak near the axis before going to zero exactly at the axis. However, in the isotropic turbulence model this happen too early due to an overestimated viscosity as the swirl approaches the axis. On the contrary, the RSM model is able to catch the strong rotational flow near the axis and the final thin rotational boundary layer very near the engine axis. The fact that the K-ω SST model destroys the swirl component in the recirculation zone determine the absence of a sufficient turbulence and mixing of reactants and the consequent low temperature and heat flux to the fuel surface. On the contrary, the RSM model predicts correctly a strong peak of the heat flux in the region where ONERA and the previous researchers found a peak of regression rate.

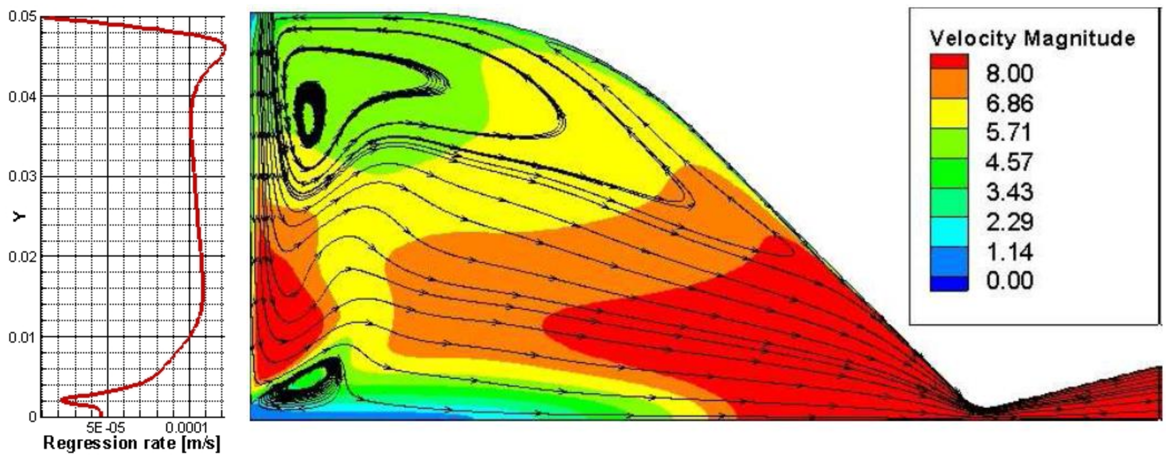

Figure 15: UNIPD simulation with conventional k-ω SST model, note the presence of the central recirculation on the fuel surface, but its low corresponding regression rate.

DOI: 10.13009/EUCASS2019-105

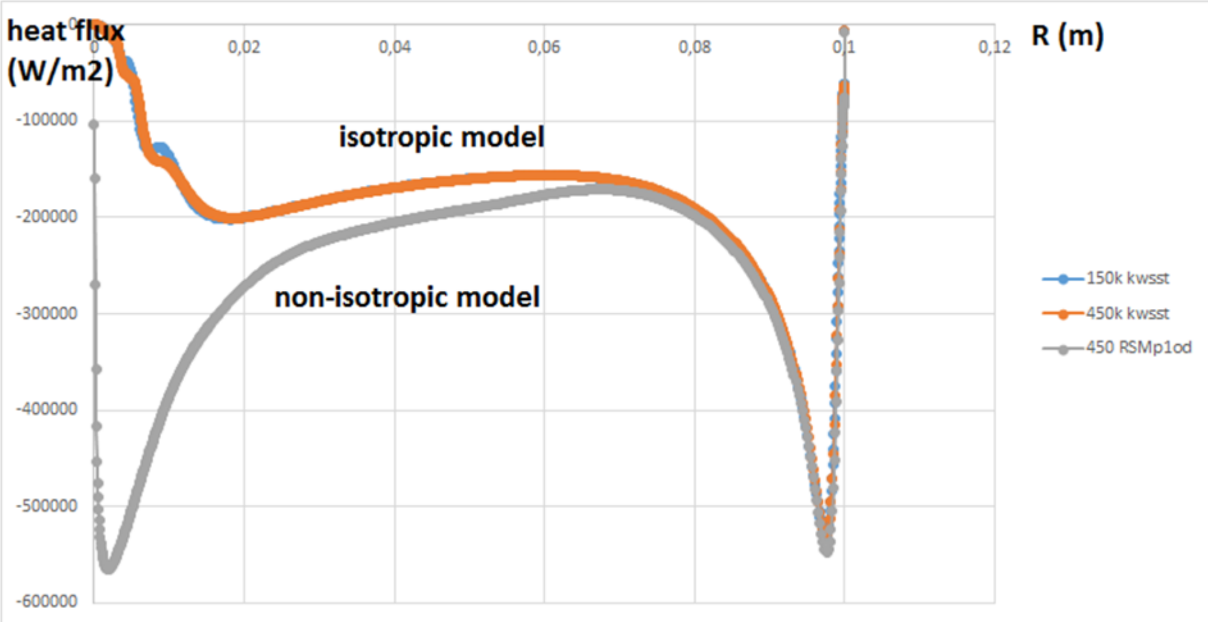

Figure 16: Heat flux on the fuel surface, comparison between different turbulence models.

The following step has been to perform combustive simulations with the new turbulence model. Unfortunately, the RSM model is much less robust than the K-ω SST model and requires a much more refined mesh. With the current resources, even after many attempts, it was not possible to perform a successful full 3D combustive simulation of the MHYCAS engine with the RSM model. However, the previous comparison suggest the possibility that the original K-ω SST model fails near the axis but could still makes useful predictions on the global motor performance an heat transfer at the external walls, particularly considering that the area at the centre is only a small fraction of the whole circular fuel surface. Moreover, previous simulations of vortex hybrid rockets performed by UNIPD predicted global performance with good accuracy even if the swirl number was technically over the limit of the isotropic turbulence model [12-17]. Based on these thoughts, the original turbulence model used by UNIPD during the HYPROGEO program has been validated on ONERA experiments. The selected test cases have been the MHYCAS 16 & 17. The nozzle throat diameter was 9.5 mm in both cases. The fuel surface before the test was flat. In the MHYCAS 16, two injectors were fully open; while in the MHYCAS 17 two injectors were partially open (1/3 of the area).

Case	**Oxidizer flow (g/s)**	**Experimental chamber pressure (bar)**	**CFD pressure w/o UDF (bar)**	**CFD pressure with UDF (bar)**	**Experimental regression rate (mm/s)**	**CFD regression rate (mm/s)**
MHYCAS 16	36.15	7.67	7.35	7.69	0.102	0.110
MHYCAS 17	30.60	7.02	7.27	7.42	0.137	0.139

Table 2: Summary of the simulated cases

The simulations with the standard K-ω SST model are able to determine chamber pressure with an accuracy of +/- 6%. The average regression rate is predicted by the UDF with an accuracy of +/- 10%. Due to the low robustness of the RSM model and the improvement of the computational capabilities, it is suggested that the best solution for the future should be to shift to a LES type of turbulence treatment.

DOI: 10.13009/EUCASS2019-105

5. Conclusions

Conventional hybrid rocket motors are not suitable for low thrust, very long burning-time spacecraft applications because of the time-dependent shift in mixture ratio and associated variations in grain shape. In the Framework of the European Commission's H2020 HYPROGEO program, an innovative combustion chamber has been proposed to explore the application of hybrid propulsion as a replacement for current liquid propellant apogee engines. Such a combustion chamber, which is isochoric, has a length-to-diameter ratio of the order of one. This unconventional hybrid rocket is based on an end-grain solid fuel burning axially in conjunction with a lateral swirled injection of oxidizer.
The design and the development of this new architecture of hybrid engine require the knowledge of the internal flow field. A customized commercial CFD code has consequently been used to perform multiple simulations with the aim of understanding the combustion behaviour in the isochoric chamber and predicting the main motor parameters like regression rate and wall heat transfer.
The numerical tools used have been previously validated for conventional hybrid rocket motors. However, the HYPROGEO motor characteristics depart significantly from those of a classical hybrid, both in terms of geometry, fluid flow behaviour and operating conditions. Therefore, these numerical simulations present new challenges especially in the application of new physics within the numerical model.
A new test rig, based on the same design that the one considered for the hybrid engine compatible with the satellite requirements, has been manufactured and tested in order to assess dedicated point such as ignition, operating conditions, etc. and to provide a dedicated experimental database to validate the numerical simulations.
The results of the investigation is that the isotropic turbulence model chosen for the standard simulations is not fully compatible with the selected swirled injection. The numerical simulations completely failed to predict a peak of the regression rate in the centre of the fuel grain as shown by the experiments. Later simulations with a non-isotropic turbulence model were able to catch the peak of the heat flux in that region. The standard isotropic model produces too much viscosity and too less turbulence near the centre compared with the non-isotropic model. However, the results of the two types of simulations are similar far from the axis of the engine. The standard simulations were still correct in predicting the global behaviour and performance. The simulations with the standard turbulence model were able to determine chamber pressure with an accuracy of +/- 6%. The average regression rate was predicted with an accuracy of +/- 10%. Due to the low robustness of the RSM model and the improvement of the computational capabilities, it is suggested that the best solution for the future should be to shift to a LES type of turbulence treatment.

4. Acknowledgments

This project has received funding from the European Union's Horizon 2020 research and innovation program under grant agreement No 634534 entitled "HYPROGEO - Hybrid Propulsion Module for Transfer to GEO Orbit".
The authors would like to thank Karine Odic and Anthony Lecossais (Airbus Defence & Space - TLS) who have been the project managers of the HYPROGEO project together with the other partners of the consortium (in particular DELTACAT and VKI in WP2 and NAMMO in WP3).
The authors would like to thank Martina Faenza (NAMMO Raufoss) for the support with the UDF.

References

[1] Project: HYPROGEO, EC H2020 Project Number 634534, Hybrid Propulsion Module for Transfer to GEO Orbit, 2015 – 2018.
[2] Odic K., Lestrade J.-Y., Verbene O., Ryan J., Christ P., de Crombrugghe G. (2016). HYPROGEO Hybrid Propulsion: Project Objectives and Coordination. Space Propulsion 2016 Proceedings, Rome, Italy.
[3] Lecossais A, Bavestrello H., Odic K., Ducerf F., Martin F., Ryan J., MacDonald M., de Crombrugghe G. (2016). HYPROGEO Hybrid Propulsion: Potential Applications & Technical Challenges. Space Propulsion 2016 Proceedings, Rome, Italy.
[4] Faenza M., Barato F., Lazzarin M. and Pavarin D., (2015). Hybrid Rocket Motors Regression rate Prediction trough CFD Simulations. EUCASS 2015 Proceedings, Krakow, Poland.
[5] Carmicino, C., and Russo Sorge, A. (2003). Investigation of the Fuel Regression Rate Dependence on Oxidizer Injection and Chamber Pressure in a Hybrid Rocket. AIAA Paper 2003-4591.
[6] Carmicino, C., Russo Sorge, A, (2005). Role of Injection in Hybrid Rockets Regression Rate. In: Journal of Propulsion and Power, Vol. 21, No. 4.
[7] Carmicino, C., Russo Sorge, A., (2006). Influence of a Conical Axial Injector on Hybrid Rocket Performance. In: Journal of Propulsion and Power, Vol. 22, No. 5.

DOI: 10.13009/EUCASS2019-105

[8] Carmicino, C., Orlandi, O., Russo Sorge, A., Dauch, F., De Amicis, R., De Rosa, M., (2009). Basic Aspects of the Hybrid Engine Operation. In: 45th AIAA Joint Propulsion Conference & Exhibit, AIAA-2009-4937, Denver, CO.

[9] Barato F., Paccagnella E., Venturelli G., Scarpa M., Picano F., Pavarin D., Lestrade J.-Y. (2016). Numerical Simulation of an Isochoric Combustion Chamber for Hybrid Rocket Propulsion. Space Propulsion 2016 Proceedings, Rome, Italy.

[10] Bellomo N., Lazzarin M., Barato F. and Grosse, M. (2010). Numerical Investigation of the Effect of a Diaphragm on the Performance of a Hybrid Rocket Motor. In: 46th AIAA/ASME/SAE/ASEE Joint Propulsion Conference & Exhibit. AIAA-2010-7033, Nashville, TN, USA.

[11] Chiaverini M. J. (2007). Review of Solid-Fuel Regression Rate Behavior in Classical and Nonclassical Hybrid Rocket Motors. In: Fundamentals of Hybrid Rocket Combustion and Propulsion. Ed. by M. J. Chiaverini and K. K. Kuo. Vol. 218. Progress in Astronautics and Aeronautics.

[12] Barato F., Faenza M., Bellomo N., Lazzarin M., Bettella A. and Pavarin D. (2012). Numerical Simulations of an H2O2 Vortex Hybrid Rocket Motor. In: 3rd Space Propulsion Conference Proceedings.

[13] Bellomo N., Barato F., Faenza M., Lazzarin M., Bettella A. and Pavarin D. (2013). Numerical and Experimental Investigation of Unidirectional Vortex Injection in Hybrid Rocket Engines. In: Journal of Propulsion and Power Vol. 29, No. 5 pp. 1097-1113.

[14] Bellomo N., Faenza M., Barato F., Bettella A. and Pavarin D. (2012). The “Vortex Reloaded” Project: Numerical Investigation on Fully Tangential Vortex Injection in N2O-Paraffin Hybrid Motors. In: 48th AIAA/ASME/SAE/ASEE Joint Propulsion Conference & Exhibit. AIAA-2012-3903, Atlanta, GA, USA.

[15] Bellomo N., Faenza M., Barato F., Bettella A. and Pavarin D. (2012). The “Vortex Reloaded” Project: Experimental Investigation on Fully Tangential Vortex Injection in N2O-Paraffin Hybrid Motors. In: 48th AIAA/ASME/SAE/ASEE Joint Propulsion Conference & Exhibit. AIAA-2012-4304, Atlanta, GA, USA.

[16] Paccagnella E., Barato F., Pavarin D. and Karabeyoglu A. (2015). Scaling of Hybrid Rocket Motors with Swirling Oxidizer Injection – Part 2. In: 52nd AIAA/ASME/SAE/ASEE Joint Propulsion Conference & Exhibit. AIAA-2016-4750, Salt Lake City, UT, USA.

[17] Paccagnella E., Barato F., Pavarin D. and Karabeyoglu A. (2017). Scaling Parameters of Swirling Oxidizer Injection in Hybrid Rocket Motors. In: Journal of Propulsion and Power Vol. 33, No. 6 pp. 1378-1394.